

STRUCTURES ON RANDOM ELASTIC SUPPORTS

PART 2 : THIN PLATES

Hisham Hamdi Abdelmohsen

Structural Engineering Department
Faculty of Engineering, Alexandria University,
Alexandria, 21544-Egypt

ABSTRACT

The article deals with thin plates rest on random elastic supports. Supporting soil domain is modeled by the expected mean value and the coefficient of variation (COV), of the coefficient of the subgrade reaction (K). K is assumed to follow a homogenous low pass normal distribution. The solution to the plate's governing differential equation, via finite difference numerical approximation method, has led to probabilistic distributions for plate's deflection, and consequently the induced stresses. Resulting distributions are expressed in terms of the Probability Density Function (PDF), and the Cumulative Distribution Function (CDF) for each attentive variable. Variation of COV for K and the load was exercised in the analysis.

Finally, the probability of failure is instituted for various material strength distributions. Simple failure model relates principle stresses to strength values was mastered in the analysis. A new method based on the probabilistic nature of the coefficient of subgrade reaction and plate's material strength, is advanced for the design of thin plates rest on random elastic support.

Keywords: Thin Plates, Random Elastic Support, Statistical Design, Probability of Failure.

NOMENCLATURE

CDF	Cumulative distribution function
	$F_X(x)$ is the probability that X takes a value equals to or less than x, Benjamin [1]
COV	Coefficient of variation = SD/EX
E_s	Elastic modulus for supporting foundation (MPa)
E_p	Elastic modulus for plate's material (MPa)
D	Flexural rigidity (MN.m ²)
EX	Expected mean value
K	Coefficient of subgrade reaction (MN/m ³)
L_x	Plate's length in x direction (m)
L_y	Plate's length in y direction (m)
M_x	Bending moment in x direction (MN.m)
M_y	Bending moment in y direction (MN.m)
n	Number of experiments
PDF	Probability density function
	$f_X(x)$ is the probability that X is in the interval x to (x+dx), Benjamin [1]
q	Loading intensity
SD	Standard deviation, Benjamin [1]
	$\sqrt{\frac{1}{n} \left(\sum_{i=1}^n x_i^2 - n EX^2 \right)}$
w	Deflection (m)
x_i	The ith observed value

ν	Plate's Poisson ratio
σ_x	Normal stress in the x direction (MPa)
σ_y	Normal stress in the y direction (MPa)
σ_1	Major principal stress (MPa)
σ_2	Minor principal stress (MPa)
τ_{xy}	Shear stress (MPa)

INTRODUCTION

Subsequent to the study included in Abdelmohsen [2], that analyzed beams rest on random elastic support, we have extended the investigation program here to thin plates. Our effort focused on mastering the results featured for the beams, to cover a two dimensional problem conceived in thin plates. The solution steps are analogous to the beams. The governing differential equation of a thin plate supported by elastic foundation is transformed into finite difference approximation scheme, James et al. [3]. The coefficient of subgrade reaction is assigned a random value based on an assumed expected mean and standard deviation values, manipulating Monte Carlo simulation technique, Press et al. [4], Greco [5], and Song [6]. Consequently, there is a distinct K value at each finite difference grid node, and for each running experiment. Thus, the symmetry

each running experiment. Thus, the symmetry of the problem is spoiled, and the whole plate should be engaged in the analysis. One expected mean value for K is mastered in the entire analysis, that simulates medium/dense sand. K and the uniform loading are allowed to have various COV, of values up to 0.20.

THEORETICAL MODEL

The governing differential equation for a thin plate supported by an elastic foundation is given as, Bowles [7]

$$\frac{\partial^4 w}{\partial x^4} + 2 \frac{\partial^4 w}{\partial x^2 \partial y^2} + \frac{\partial^4 w}{\partial y^4} = -\frac{kw}{D} + \frac{P}{D \partial x \partial y} \quad (1)$$

The above equation is discretized using finite difference central approximation algorithm. The random value for the coefficient of subgrade reaction is then generated, from assigned values for the expected mean and standard deviation. Monte Carlo simulation routine, (Press et al. [4]), manipulates those values to construct a set of K values correspond to each imitated experiment. The finite difference equation with random K values, plate stiffness, and external loading is solved using successive over relaxation technique, with a specified value for convergence accuracy. Internal stresses are then generated from the deflection solution at each node located in the plate domain, as seen in Appendix A. Probability density functions, PDF, as well as the Cumulative Distribution Functions CDF for the deflection, and each of the induced stresses are easily secured, once the deflection solution is achieved for each experiment.

In general, both the strength R, and the loading stress S, of a soil structure are random variables. The ratio of the mean values of R and S is so called the central factor of safety, CFS, and it is generally different from F_s , as the later depends on the choice of the estimators R_o and S_o . The difference between R and S is also a random variable called the safety margin, SM ($SM = R - S$).

Failure of the structure occurs when the SM has negative value, i. e. ($SM = R - S < 0$). The probability of the occurrence of this event is equal to the probability of failure, $P_f = P(\text{Failure}) = P(SM < 0)$. If $f_R(R)$ and $f_S(S)$ denote the probability density functions of strength R and loading stress S, respectively, the expression for the probability of failure P_f becomes, Athanasiou-Grivas [8]

$$P_f = \int_{-\infty}^{\infty} F_R(S) f_S(S) dS \quad (2)$$

in which $F_R(S)$ is the cumulative distribution function of the strength.

To comply with the above equation, the PDF of the loading stress is been generated for the major principal stresses σ_1 and σ_2 , calculated by the equation, Dally and Riley [9]

$$\sigma_{1,2} = \left(\frac{\sigma_x + \sigma_y}{2} \right) \pm \sqrt{\left(\frac{\sigma_x - \sigma_y}{2} \right)^2 + \tau_{xy}^2} \quad (3)$$

RESULTS

The following parameters are exercised in the analysis:

For the supporting foundation, Coefficient of subgrade reaction K

Expected mean value = 300 MN/m³ (simulation for Medium/Dense sand)

Coefficient of variation COV = Variable = 0.10, and 0.20, Lee et al. [10] and Baecher [11].

For the thin plate

Length in x direction $L_x = 1.00$ m

Length in y direction $L_y = 1.00$ m

Thickness = 0.10 m

Elastic modulus $E_p = 21.0$ GPa, Bowles [7]

Poisson's ratio = 0.25, Bowles [7]

The plate is assumed to be simply supported with the following boundary conditions, (Shames, and Dym [12])

At $x = 0$ and $x = L_x$: $w = M_x = 0$

At $y = 0$ and $y = L_y$: $w = M_y = 0$

For the numerical operation, (James et al [3], Press et al. [4])

Number of node points in x direction = 20

Number of node points in y direction = 20

Convergence factor = 1.E-8

Relaxation factor = 1.50

For the external loading

Uniformly distributed load = 1.E-2 MPa

Coefficient of variation COV = Variable = 0.10, and 0.20.

Figures 1 through 4 demonstrate the CDF for the deflection and the induced stresses. Each figure illustrates two curves, curve 1 for the maximum value that ever takes place, whilst curve 2 represents the minimum value that ever results. Each curve is procured at different node numbers. Curves for other nodes shall fall between these two boundary curves. The above figures are exclusive to perform the complete probabilistic design, with the present of the compelled degree of confidence.

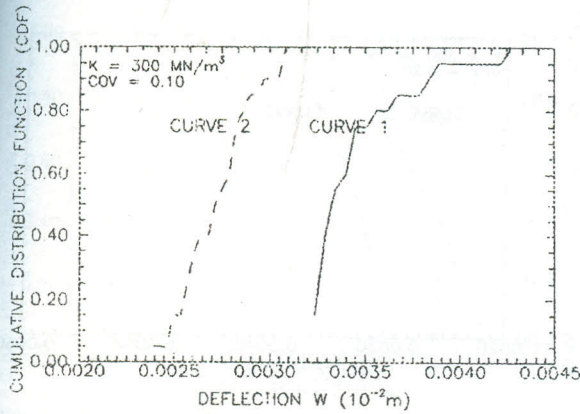


Figure 1 CDF for maximum and minimum deflection

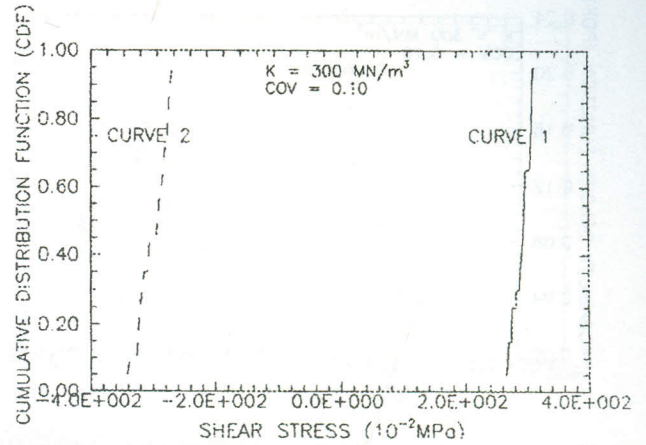


Figure 4 CDF for Maximum and minimum shear stress values

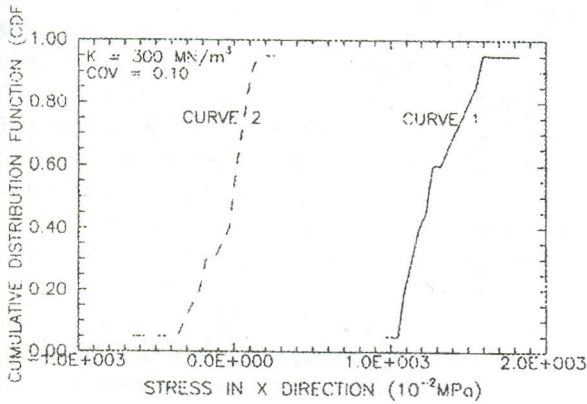


Figure 2 CDF for maximum and minimum normal stress values in x direction

Results reported in Figures 5-8, substantiate the previously derived conclusion, Abdelmohsen [2] The probability density functions for all concerned variables are normal functions with different standard deviations and coefficient of skewness. These curves are derived at the same node points at which the maximum and the minimum values of each measured variable are reported. Afresh, the rest of the curves shall fall between these two extreme curves. To capture the impact of the COV value of K, on the magnitude, and the shape of CDF curves, Figures 9-12 are compiled, for new COV value, twice the previously reported values of Figures 1 to 4. In summary, at the same degree of confidence, the higher is the COV in K, the more is the resulting deflection, and stresses.

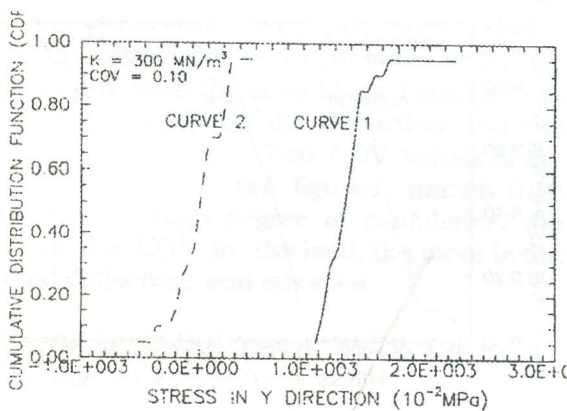


Figure 3 CDF for maximum and minimum normal stress values in Y direction

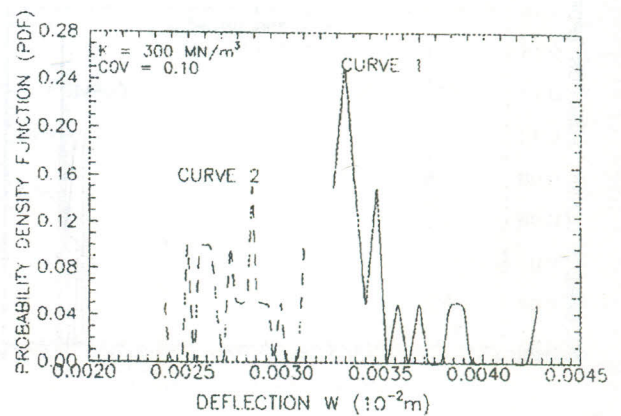


Figure 5 PDF for maximum and minimum deflection

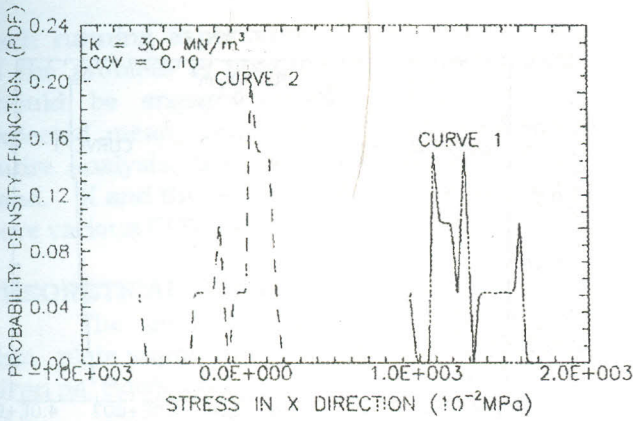


Figure 6 PDF for Maximum and minimum normal stress values in x direction

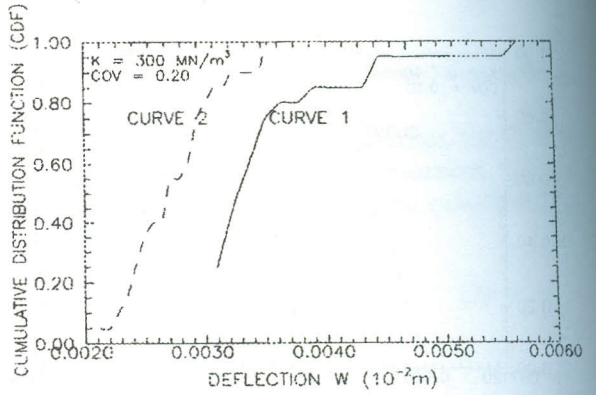


Figure 9 CDF for maximum and minimum deflection

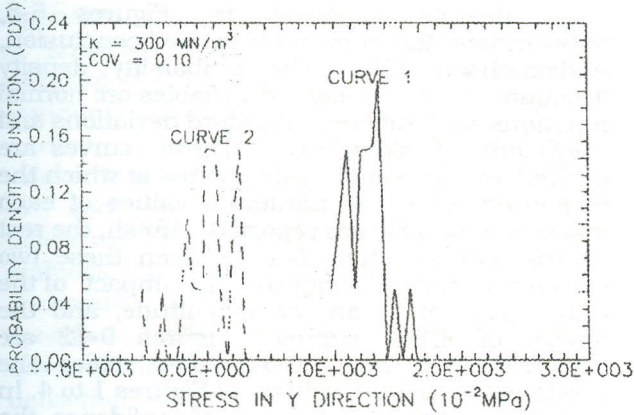


Figure 7 PDF for maximum and minimum normal stress values in Y direction

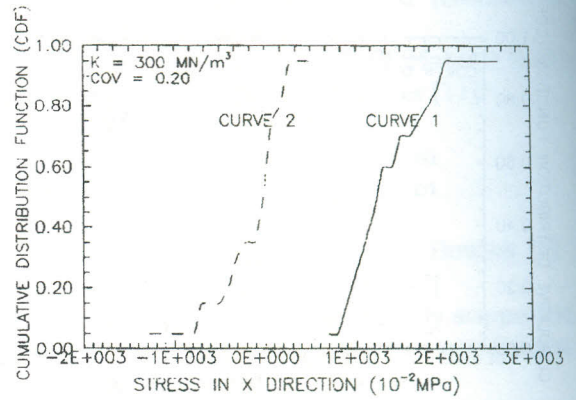


Figure 10 CDF for maximum and minimum normal stress values in X direction

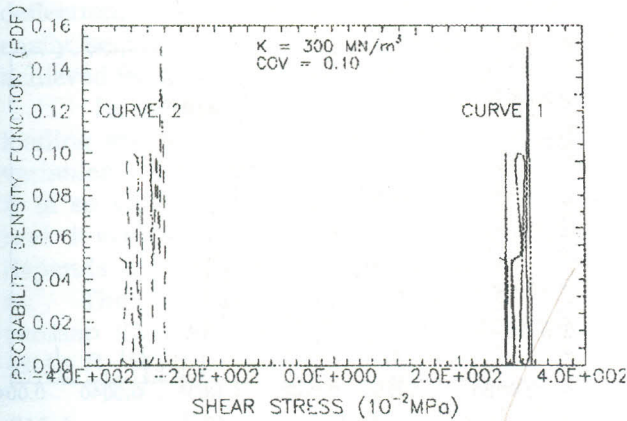


Figure 8 PDF for maximum and minimum shear stress values

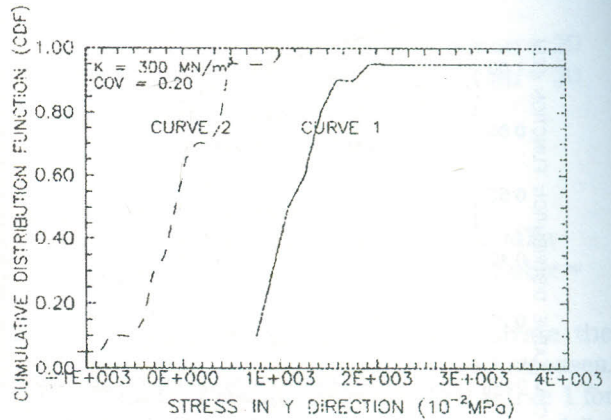


Figure 11 CDF for maximum and minimum normal stress values in Y direction

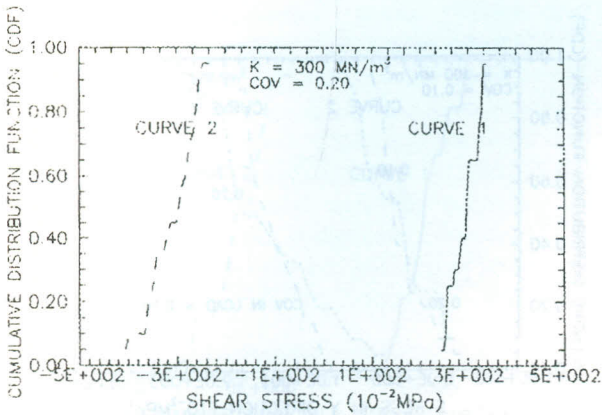


Figure 12 CDF for Maximum and minimum shear stress values

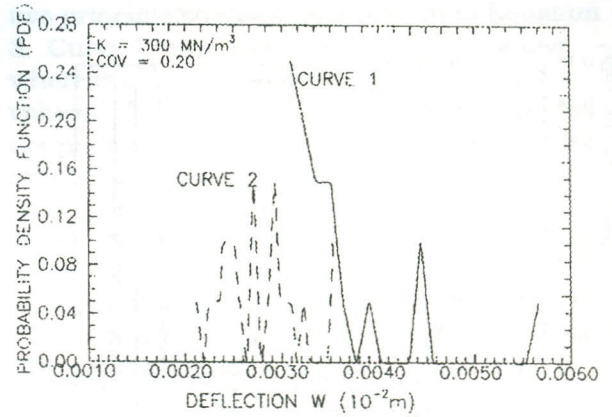


Figure 13 PDF for maximum and deflection

For example, the maximum deflection at 80% degree of confidence is $3.65E-5$ m when COV is 0.10, and its $3.8E-5$ when COV is 0.20. The same conclusion extends to stresses, e. g. the stress in the x direction is $1.5E+1$ MPa for a degree of confidence of 80%, and COV of 0.10, whilst its $1.8E+1$ MPa for the same degree of confidence and for COV of value equals to 0.20. It is easy to show that, the same argument is applied to the rest of the stresses as seen in Figures 11 and 12. Figures 13 to 16 are intended to confirm the shape of the PDF and to reveal the effect of the COV of K on the values of expected mean, standard deviation, and coefficient of skewness. The other important parameter that needs special investigation, is the COV in the applied load. This is certainly an eminent parameter, with a high existing probability associated to the presence of the live loads coupled with the dead loads. Figures 17 to 20 show the CDF for the deflection and the stresses, respectively. Two COV values of the load are depicted in the figures, namely 0.10 and 0.20. At high degree of confidence, the higher is the COV in the load, the more is the expected deflection, and stresses.

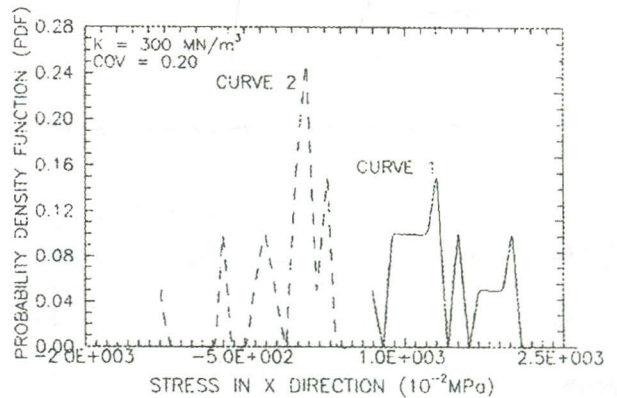


Figure 14 PDF for maximum and minimum normal values in Y direction

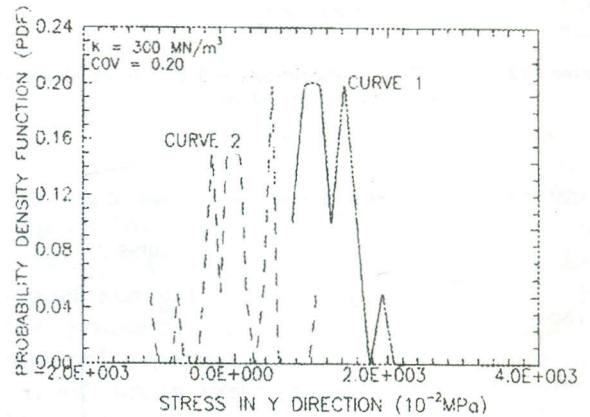


Figure 15 PDF for maximum and minimum normal stress values in Y direction

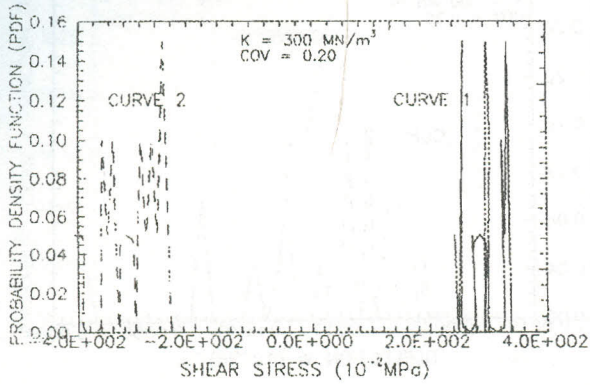


Figure 16 PDF for maximum and minimum shear stress values

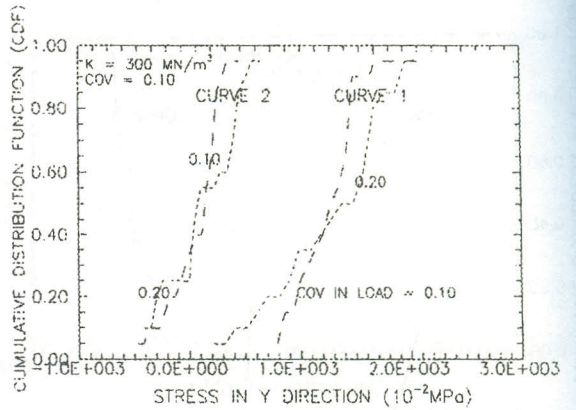


Figure 19 CDF for maximum and minimum normal stress values in Y direction including load variation

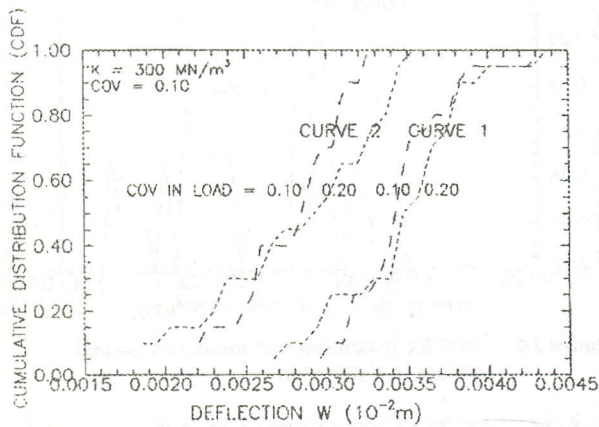


Figure 17 CDF for maximum and minimum deflection including load variation

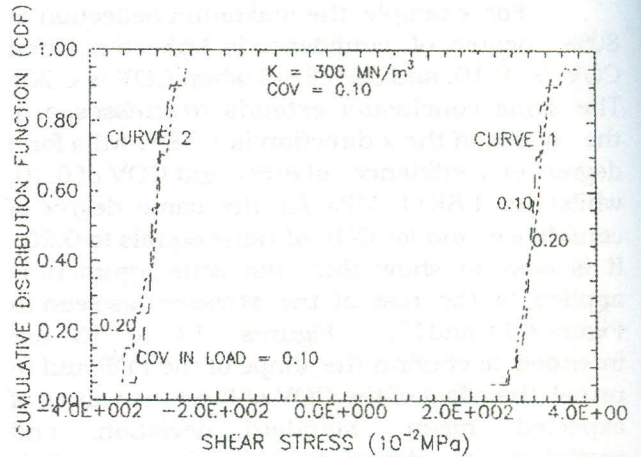


Figure 20 CDF for maximum and minimum shear stress values including load variation

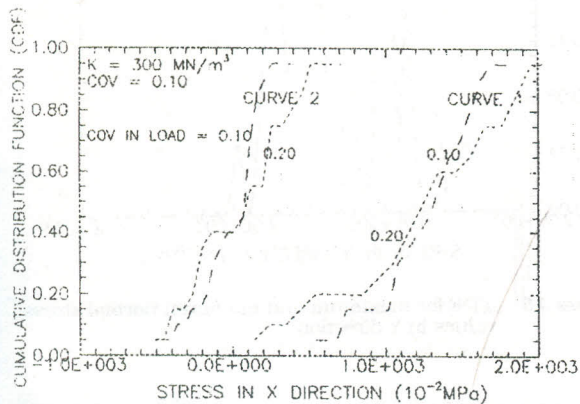


Figure 18 CDF for maximum and minimum normal stress values in X Direction including load variation

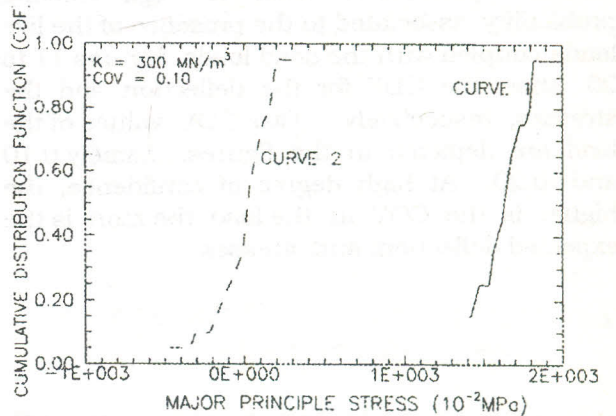


Figure 21 CDF for maximum and minimum major principal stress

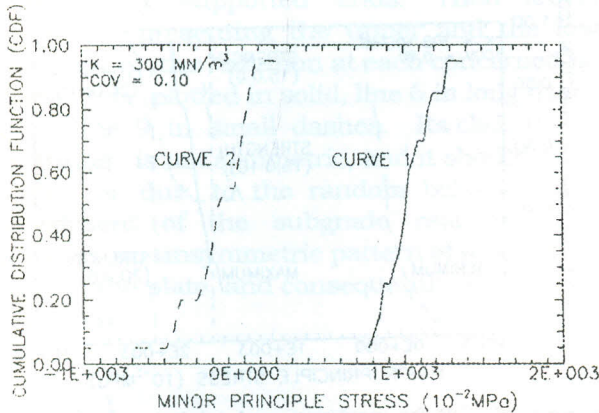


Figure 22 CDF maximum and minimum minor principle stress

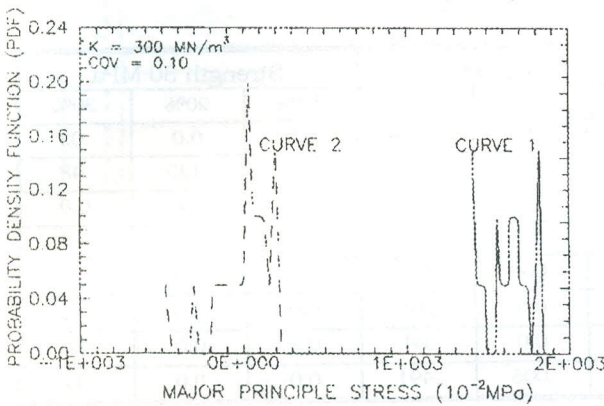


Figure 23 PDF maximum and minimum major principal stress

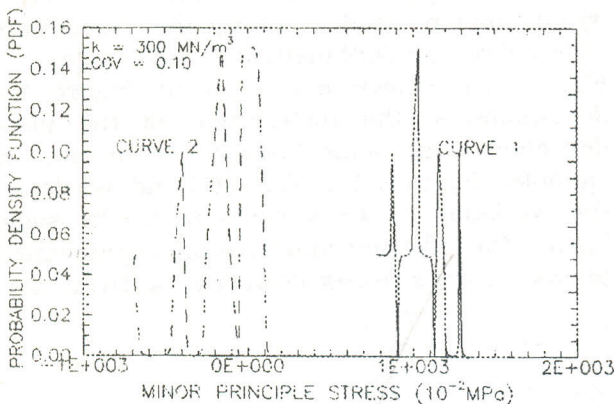


Figure 24 PDF maximum and minimum minor principal stress

This conclusion is in agreement to the effect of the COV in K on the above mentioned variables. Figures 21 and 22 show the CDF for the maximum and the minimum values for the

two principle stresses, procured from Equation 3. Curve 1 represents the maximum values, whereas curve 2 illustrates the minimum values. The PDF for the two principle stresses are plotted in Figures 23 and 24, and ready for implementation of Equation 2.

Figure 25 illustrates the strategy for performing the integration shown in Equation 2. If both the load density function and the strength cumulative function have simple analytical expressions, an integration such as the one of Equation 2. could be secured analytically.

However, as we see from Figure 25 both expressions are complex, and thus numerical integration, (James et al. [3], and Press et al [4]), is a must.

Table 1 summarizes the probability of failure results, acquired from Equation 2. versus the strength/variation (COV in the strength). Strength values instituted in the table are selected with the aid of Figure 26, which is compiled from Figure 21. Numbers between paragnathus define the expected mean and the COV values. Figure 26 ruled out the use of any material of expected mean strength less than 20 MPa.

The Table provides all pertaining information for the statistical design for thin plates of particular dimensions and stiffness. Column 1 is the node number where the cross listed variable in column 2 is critical. Three various material strengths, Egyptian Code for Design and Executing Reinforced Concrete Structures [13], demarcated by the expected mean values are used for simulation purpose. For each material's strength, we have assigned different COV values, rambled between 0 and 0.30. The demonstrated Table serves as a model example for the statistical design. For the problem in hand, one would select a material expected mean strength to be 25 MPa, whilst, limits the value of COV to be 10%. Material of less expected mean value, and of COV value below the 10%, is also a potential candidate.

A table similar to Table 1 is suggested to be compiled for each design problem, to host all possible combination of the expected mean values and COVs for various available material. As such, stresses and strengths are connected through probability of failure, rather than safety factor.

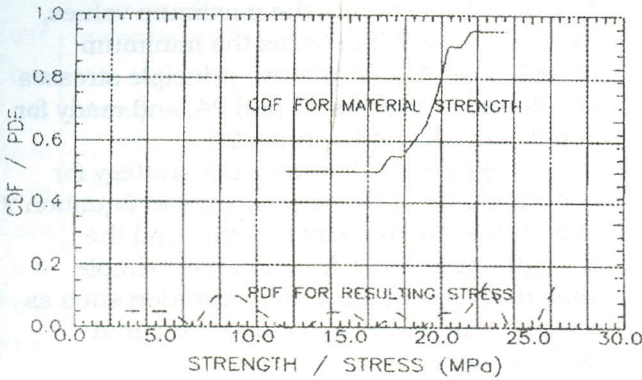


Figure 25 CDF for material strength & PDF for resulting stress

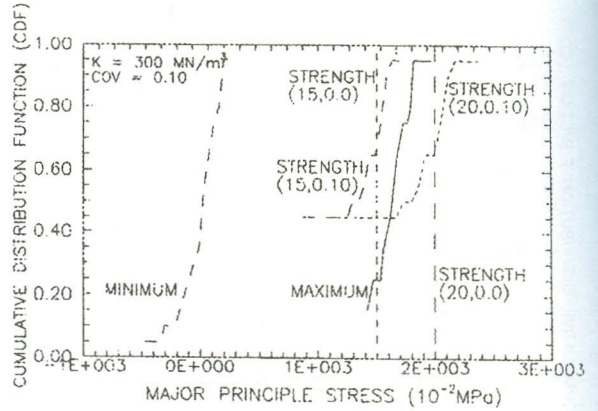


Figure 26 CDF for maximum and minimum major principle stress and material's strength

Table 1. Probability of failure for various material's expected mean strengths and strength's variations (COV)(NN= node number, CRV= critical resulting variable, Min. = minimum, Max. = maximum)

NN	CRV	Strength 20 MPa			Strength 25 MPa			Strength 30 MPa		
		10%	20%	30%	10%	20%	30%	10%	20%	30%
3.3	Min. w	.113	.313	.488	0.0	.003	.488	0.0	0.0	.03
3.18	Max. τ_{xy}	.317	.492	.493	0.0	.475	.493	0.0	.125	.48
7.4	Min. σ_y	0.0	0.0	0.0	0.0	0.0	0.0	0.0	0.0	0.0
9.	Max. w	0.0	0.0	0.0	0.0	0.0	0.0	0.0	0.0	0.0
13.18	Max. σ_x	0.0	.225	.475	0.0	.003	.475	0.0	0.0	.27
16.14	Min. σ_x	0.0	0.0	0.0	0.0	0.0	0.0	0.0	0.0	0.0
18.12	Max. σ_y	0.0	.175	.040	0.0	0.0	.04	0.0	0.0	0.0
18.18	Max. τ_{xy}	.006	.44	.49	0.0	.005	.491	0.0	0.0	.12

CONCLUSION

We have demonstrated the influence of the random nature of the coefficient of subgrade reaction on the induced deflection and stresses in thin plates resting on elastic support. At the same degree of confidence, the increase in the variation of both the coefficient of subgrade reaction and the applied loads causes an increase in all the resulting values. Based on the probabilistic analysis, a new method is proposed to perform structure design for thin plates resting on random elastic foundation. The method relies the probability of failure procured from strength distribution and the resulting maximum stresses. Yet, it rules out the role of the factor of safety in transforming the ultimate strength values into permissible ones.

APPENDIX A

This Appendix is assembled to substantiate the solution of the governing

differential Equation 1, in the Finite Difference approximation model, using the Successive Over Relaxation SOR method, Press et al.[4]. Figure A-1 shows plate's layout. Figure A-2 demonstrates the distribution of the plate deflection along some lines ($y = \text{constant}$, x is variable). Figures A-2, A-3, A-4 and A-5 depict the variation of the stresses along the same lines. The following equations are implemented to procure the stresses, (Shames and Dym[12])

$$\sigma_x = -\frac{E_p z}{1-\nu^2} \left(\frac{\partial^2 w}{\partial x^2} + \nu \frac{\partial^2 w}{\partial y^2} \right) \quad (A.1)$$

$$\sigma_y = -\frac{E_p z}{1-\nu^2} \left(\frac{\partial^2 w}{\partial x^2} + \nu \frac{\partial^2 w}{\partial y^2} \right)$$

$$\tau_{xy} = -\frac{E_p z}{1+\nu} \frac{\partial^2 w}{\partial x \partial y}$$

Where Z is the distance between the plate neutral axis, and the point of interest.

In the above reported figures, nodes 1 and 20 are imaginary, introduced to simulate

the simply supported ends. There are two curves representing the upper and the lower bounds of the solution at each concerned line. Line 3 is plotted in solid, line 6 in long dashes, and line 9 in small dashes. Its clear that the solution is not symmetric, and it should not be. This is due to the random behavior of the coefficient of the subgrade reaction K , that creates an unsymmetric pattern of soil response below the plate, and consequently, the resulting solution.

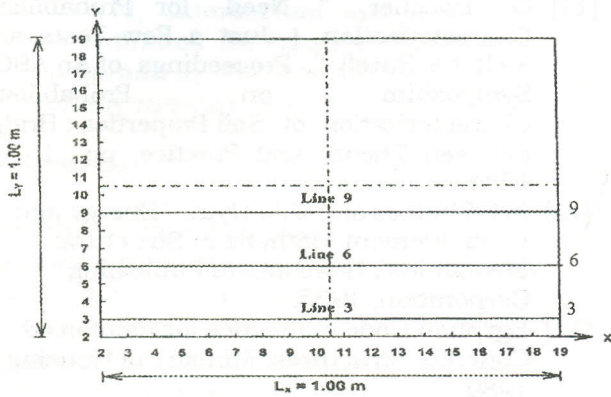


Figure A-1 Plate layout

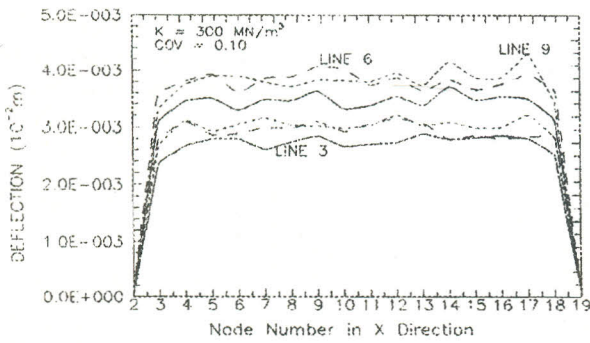


Figure A-2 Plate deflection

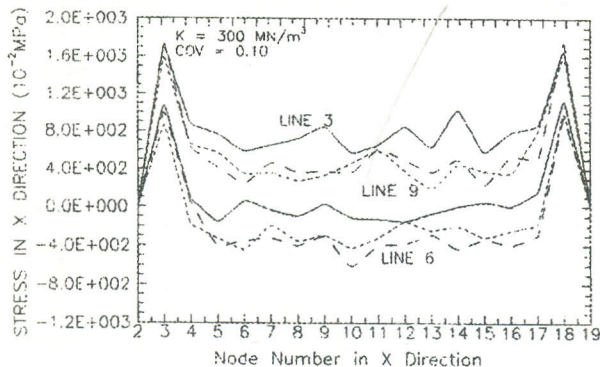


Figure A-3 Plate stresses in X direction

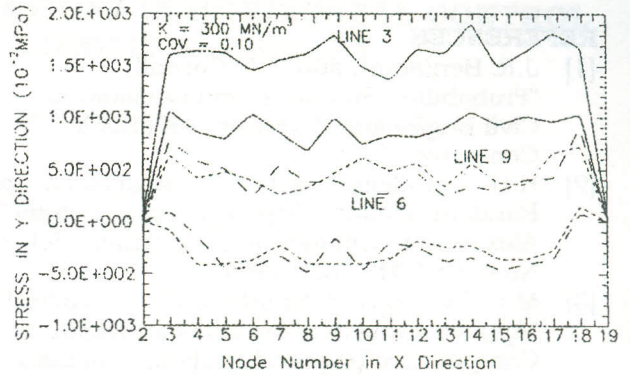


Figure A-4 Plate stresses in Y direction

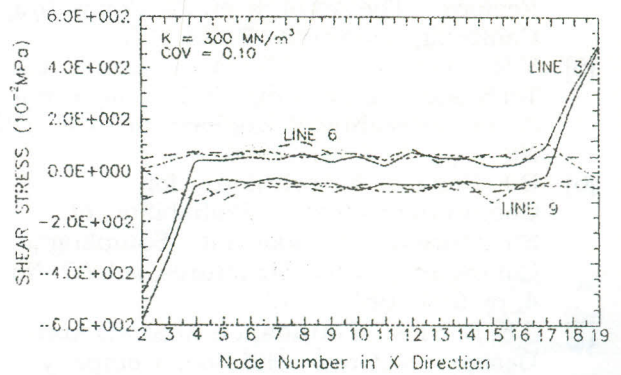


Figure A-5 Plate shear stresses

This insinuates that, the whole plate domain should be discretized, rather than one quarter of the plate, similar to common plate problems. All quoted figures confirm the accuracy of the solution. Yet, they show the influence of the coefficient of the subgrade reaction, if a 10% coefficient of variation exists due to the uncertainty born in K values. For instance, the maximum deflection along line 6 changes between $3.0E-5$ to $4.0E-5$, with 30% increase between the two values. Similar conclusion is reached by looking at stress figures. The stresses in the x direction induced along lines 6 and 9, for example, switch from negative (lower bound), to positive (upper bound). Furthermore, the stresses in the y direction alter by about 50% along line 3, and almost doubled along lines 6 and 9. Yet, they changed signs. The shear stresses are in no different status. They are too, suffered by the variation in the K magnitudes, in both values and signs.

REFERENCES

- [1] J.R. Benjamin, and C.A. Cornall, "Probability, Statistics, and Decision for Civil Engineers", McGraw - Hill Book Company, 1970.
- [2] H.H. Abdelmohsen, " Structures on Random Elastic Support, Part 1: Beams ",, Alexandria Engineering Journal, Vol.36, No.4, pp.C317-324, 1997.
- [3] M.L. James, G.M. Smith and J.C. Wolford, "Applied Numerical Methods for Digital Computation", Second Edition, Thomas Y. Crowell, Harper & Row Publishers, 1977.
- [4] W.H. Press, B.P. Flannery, S.A. Teukolsky and W.T. Vetterling, "Numerical Recipes - The Art of Scientific Computing ", Cambridge University Press, 1986.
- [5] V.R. Greco, " Effective Monte Carlo Technique for Locating Critical Slip Circle ", J. of Geotechnical Engineering, vol. 122, No. 7, pp. 517- 525,1996
- [6] B.F. Song, " A Technique for Computing Failure Probability of a Structure Using Important Sampling", Computers and Structures, vol. 62, No. 4, pp 659 - 665, 1997
- [7] J.E. Bowles, " Foundation Analysis And Design ", McGraw - Hill Book Company, 1988.
- [8] D. Athanasiou-Grivas, "Probabilistic Evaluation of Safety of Soil Structures", Geotechnical Engineering Division, Proceedings of American Society of Civil Engineers, Vol. 105, No. GT9, September pp. 1091 - 1095, 1979
- [9] J.W. Daily and W.F. Riely, " Experimental Stress Analysis ", McGraw - Hill Book Company, 1978.
- [10] I.K. Lee, W. White and O.G. Ingles, "Geotechnical Engineering ", Pitman Publishing Inc, 1983.
- [11] G. Baecher, " Need for Probabilistic Characterization (Just a Few Tests and we'll be Sure!) ", Proceedings of An ASCE Symposium on Probabilistic Characterization of Soil Properties : Bridge Between Theory and Practice, pp. 1 - 18, 1984.
- [12] I.H. Shames and C.L. Dym, " Energy and Finite Element Methods in Structural Mechanics", Hemisphere Publishing Corporation, 1985.
- [13] Egyptian Code of Practice for Reinforced Concrete Structures, Ministry of Housing, 1989